GTP Analogue Inhibits Polymerization and GTPase Activity of the Bacterial Protein FtsZ without Affecting Its Eukaryotic Homologue Tubulin†

Tilman Läppchen,‡ Aloysius F. Hartog,‡ Victorine A. Pinas,‡ Gerrit-Jan Koomen,‡ and Tanneke den Blaauwen*,§

Bioorganic Chemistry, Van't Hoff Institute for Molecular Sciences, University of Amsterdam, Nieuwe Achtergracht 129, 1018 WS Amsterdam, and Molecular Cytology, Swammerdam Institute for Life Sciences, University of Amsterdam, Kruislaan 316, 1098 SM Amsterdam, The Netherlands

Received December 23, 2004; Revised Manuscript Received April 4, 2005

ABSTRACT: The prokaryotic tubulin homologue FtsZ plays a key role in bacterial cell division. Selective inhibitors of the GTP-dependent polymerization of FtsZ are expected to result in a new class of antibacterial agents. One of the challenges is to identify compounds which do not affect the function of tubulin and various other GTPases in eukaryotic cells. We have designed a novel inhibitor of FtsZ polymerization based on the structure of the natural substrate GTP. The inhibitory activity of 8-bromoguanosine 5′-triphosphate (BrGTP) was characterized by a coupled assay, which allows simultaneous detection of the extent of polymerization (via light scattering) and GTPase activity (via release of inorganic phosphate). We found that BrGTP acts as a competitive inhibitor of both FtsZ polymerization and GTPase activity with a K_i for GTPase activity of 31.8 ± 4.1 μM. The observation that BrGTP seems not to inhibit tubulin assembly suggests a structural difference of the GTP-binding pockets of FtsZ and tubulin.

The cytoskeleton plays a crucial role in the organization of both eukaryotic and prokaryotic cells. Microtubules and actin filaments, the main cytoskeletal elements in eukaryotes, are highly dynamic structures which are maintained by continuous assembly and disassembly of tubulin and actin. In bacteria, dynamic assembly of the prokaryotic tubulin homologue FtsZ into a macromolecular structure called the Z ring is a central event in cell division (for recent reviews, see refs *1*−*3*). Ring formation coincides with termination of DNA replication (*4*, *5*) and is followed by recruitment of other cell division proteins (for a review, see ref *6*).

Although FtsZ shows only weak sequence homology to the eukaryotic tubulins (*7*), FtsZ and tubulin possess similar three-dimensional structures both as monomers (*8*, *9*) and when modeled onto protofilaments (*10*, *11*). Like tubulin, FtsZ is a GTPase, and its amino acid sequence includes a seven-residue GTP-binding motif [GGGTGTG] which is almost identical to the signature sequence involved in the binding of GTP by tubulins (*12*). In vitro FtsZ polymerization dynamics have been well characterized (*3*, *13*, *14*). In the presence of GTP, FtsZ assembles into thin protofilaments, which depolymerize upon depletion of GTP (*15*). Hydrolysis of GTP is Mg^{2+}-dependent and requires oligomerization of FtsZ, indicating that the active site is formed by the association of monomers (*16*, *17*).

Selective inhibitors of FtsZ polymerization, which do not affect tubulin polymerization, are interesting candidates for novel antibacterial agents and might also contribute to resolve mechanistic questions of the FtsZ polymerization dynamics (*18*). Until now, identification of small-molecule inhibitors of FtsZ was mainly accomplished by screening large chemical libraries (*18*, *19*) or numerous extracts of microbial fermentation broths and plants (*20*).

In an alternative approach, we designed a selective inhibitor of FtsZ based on the structure of its natural substrate GTP. Our search for a suitable lead compound was greatly facilitated by making use of published data on the nucleoside triphosphate specificity of tubulin (*21*, *22*) and FtsZ (*8*, *23*, *24*). For both proteins, the 2-exocyclic amino group and the 6-oxo group are essential for base recognition. In contrast, a study on the effect of various GTP analogues on microtubule assembly demonstrates that GTP derivatives with a bromine or hydroxyl group at C8 still promote tubulin polymerization (*25*, *26*). We deduced from the crystal structure of FtsZ that the C8 position of GTP might allow variation without obstructing the binding to an FtsZ monomer. In addition, we expected that binding of a C8-substituted GTP to the top of a monomer will block its ability to associate with the bottom of another monomer and form a filament.

The absence of inhibitory activity of 8-bromoguanosine 5′-triphosphate (BrGTP,[1] Figure 1) on tubulin assembly prompted us to investigate the effect of BrGTP on FtsZ polymerization. Here, we report the synthesis of BrGTP together with a thorough characterization of its inhibitory properties on FtsZ function by both electron microscopy and

† This work was supported in part by a "Vernieuwingsimpuls" grant (016.001.024, T.d.B.) of the Netherlands Organization for Scientific Research (NWO).

* To whom correspondence should be addressed. Fax: +31-20-5256271. E-mail: blaauwen@science.uva.nl.

‡ Van't Hoff Institute for Molecular Sciences.

§ Swammerdam Institute for Life Sciences.

[1] Abbreviations: BrGTP, 8-bromoguanosine 5′-triphosphate; Bu_3N, tri-*n*-butylamine; DMF, dimethylformamide; *E. coli*, *Escherichia coli*; TMS, tetramethylsilane; HEPES, 4-(2-hydroxyethyl)-1-piperazineethanesulfonic acid; MES, 2-morpholineethanesulfonic acid; EM, electron microscopy; *M. jannaschii*, *Methanococcus jannaschii*.

10.1021/bi047297o CCC: $30.25
Published on Web 05/06/2005

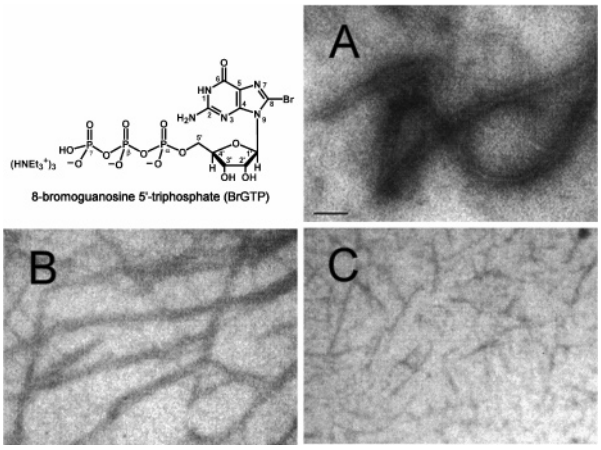

FIGURE 1: Structure of BrGTP and EM images of polymerized FtsZ formed in the presence of GTP and BrGTP. FtsZ (2.5 μM) was incubated in MES buffer (pH 6.5) supplemented with 5 mM $MgCl_2$ and 10 mM $CaCl_2$ at 30 °C, and polymerization was induced by adding 10 μM GTP (A), 8 μM GTP/2 μM BrGTP (B), or 6.6 μM GTP/3.3 μM BrGTP (C). After 2 min, samples were processed for electron microscopy. The bar is 100 nm.

a coupled assay, which simultaneously monitors the degree of polymerization and the release of inorganic phosphate. Our results demonstrate that BrGTP is a competitive inhibitor of FtsZ polymerization and GTPase activity. The identification of a GTP-derived selective inhibitor of FtsZ assembly is another step toward a better understanding of the structural differences between FtsZ and tubulin and the mechanisms governing the polymerization process.

EXPERIMENTAL PROCEDURES

Overproduction and Purification of FtsZ. FtsZ was overproduced in *E. coli* BL21(DE3) transformed with pRRE6 and purified as described earlier (*27*). Protein concentration and purity were determined by amino acid quantification (Eurosequence, The Netherlands). FtsZ was 99.4% pure.

Synthesis and Characterization of BrGTP. BrGTP was synthesized starting from guanosine. 8-Bromoguanosine was prepared by direct bromination of guanosine with bromine in water (*28*) in 85% yield. The unprotected nucleoside was then 5′-triphosphorylated by a one-pot procedure using phosphorus oxychloride and tri-*n*-butylammonium pyrophosphate in trimethyl phosphate according to a slightly modified literature procedure (*29*, *30*). In short, a solution of 8-bromoguanosine (91 mg, 0.25 mmol) in dry trimethyl phosphate (2 mL) was cooled to 0 °C, and Proton Sponge (161 mg, 0.75 mmol, 3 equiv) was added. After the resulting solution was stirred for 20 min at 0 °C, $POCl_3$ (70 μL, 0.75 mmol, 3 equiv) was added dropwise. The reaction was allowed to stir for another 2 h at 0 °C. Then a mixture of Bu_3N (0.24 mL, 1.00 mmol, 4 equiv) and 1 M $(Bu_3NH^+)_2(H_2P_2O_7^{2-})$ in DMF (1.5 mL, 1.50 mmol, 6 equiv) was added at once followed by quenching with 15 mL of 0.2 M $(Et_3NH^+)(HCO_3^-)$ after 1 min. The crude reaction mixture was lyophilized, applied to a 3 × 20 cm column of DEAE Sephadex A-25 coupled to a UV monitor with recording at 260 nm, and eluted with a linear gradient of 0.1−1.0 M NH_4HCO_3. Fractions containing the triphosphate were pooled and lyophilized overnight. Yield: 93 mg (0.14 mmol, 57%). The product was further purified by semipreparative HPLC with an Adsorbosphere nucleotide/nucleoside 7 μm column (1 × 25 cm; Alltech Associates, Inc.) equipped with the corresponding guard column and a linear gradient of 0.1 M triethylammonium acetate (eluant A) and acetonitrile (eluant B) at a 4 mL/min flow rate. Gradient details: 0−5 min, 0% B; 5−25 min, 0% → 10% B; 25−30 min, 10% B; 30−33 min, 10% → 0% B; 33−40 min, 0% B. Detection: UV absorption at 262 and 225 nm using a Pharmacia LKB VWM2141 dual diode array variable-wavelength detector. The retention time was 22.0 min and the purity >90%.

The compound was characterized by ^{1}H and ^{31}P nuclear magnetic resonance spectroscopy on a Varian Inova-500 spectrometer. ^{1}H chemical shifts are reported in parts per million relative to the peak for sodium (3-trimethylsilyl)-propionate (a water-soluble form of TMS) as an internal standard, ^{31}P chemical shifts are in parts per million relative to the peak for an external standard of 85% H_3PO_4, and coupling constants J are in hertz. ^{1}H NMR (D_2O, 499.9 MHz): δ 5.98 (d, $^3J = 6.3$, 1H, H1′), 5.38 (t, $^3J = 6.3$, 1H, H2′), 4.68 (br s, integral cannot be determined due to superposition with the water peak, H3′), 4.31 (br s, 3H, H4′, H5′). ^{31}P NMR (D_2O, 202.4 MHz, pH 5.6): δ −9.75 (br s, P_γ), −10.31 (br s, P_α), −22.22 (br s, P_β). ^{13}C NMR (D_2O, 125.7 MHz, 5 °C): δ 158.0 (C6), 153.5 (C2), 153.0 (C4), 124.3 (C8), 116.7 (C5), 89.2 (C1′), 83.7 (C4′), 70.2 (C2′), 69.8 (C3′), 64.9 (C5′).

For the biological tests, we prepared a 10 mM stock solution of BrGTP in buffer (50 mM HEPES/NaOH, pH 7.5, 50 mM KCl) using $\epsilon = 15100$ M^{-1} cm^{-1} ($\lambda_{max} = 262$ nm, pH 7). GTP was purchased from Aldrich, and a 10 mM GTP stock solution was prepared in the same way using $\epsilon = 13700$ M^{-1} cm^{-1} ($\lambda_{max} = 253$ nm, pH 7).

Electron Microscopy. FtsZ (2.5 μM) was polymerized with 10 μM GTP (Figure 1A), 8 μM GTP/2 μM BrGTP (Figure 1B), or 6.6 μM GTP/3.3 μM BrGTP (Figure 1C) at 30 °C in 100 μL of prewarmed buffer (50 mM MES/NaOH, pH 6.5, 50 mM KCl), supplemented with 5 mM $MgCl_2$ and 10 mM $CaCl_2$. After 2 min, 3 μL of the polymerization reaction was applied to a 400-mesh carbon-coated grid for 5 min, and the grid was blotted dry by placement of a filter paper to its side. The grid was subsequently negatively stained for 1 min with 3 μL of 1% aqueous uranyl acetate and blotted dry. Finally, the grids were dried for 1 h at 30 °C. The grids were viewed in a Philips 400T transmission electron microscope (a generous gift of A. Knoester, Shell Research and Technology Centre, Amsterdam). Images were taken with a cooled Princeton CCD camera using the program IP Labspectrum 3.1 (Signal Analytics Corp.).

GTPase Activity and Polymerization Studies. We simultaneously monitored the polymerization of FtsZ and its GTPase activity by combining two assays described in the literature. Polymerization was observed by 90° angle light scattering (*23*), and the GTPase activity by a coupled assay for phosphate release (*16*). Briefly, the assay was performed in a stirred quartz cuvette that was maintained at 37 °C by a circulating water bath using a PTI QuantaMaster 2000-4 fluorescence spectrophotometer (Photon Technology International, New York), with λ(excitation) = 295 nm, λ(emission 1) = 299 nm, and λ(emission 2) = 390 nm. Excitation slit widths were 2 nm and emission slit widths 6 nm. The cuvette contained 5 mM $MgCl_2$, 50 mM KCl, and 200 μM 7-methylguanosine, 0.3 unit/mL nucleoside phosphorylase,

9 μM FtsZ, and 50 mM HEPES/NaOH, pH 7.5, in a total volume of 1.3 mL. After a baseline was recorded for 60 s, polymerization was induced by addition of GTP with final cuvette concentrations between 7.5 and 240 μM. The measurement was paused during the addition process, which generally took less than 5 s. Polymer formation of FtsZ was measured by 90° angle light scattering at 299 nm, and phosphate release from GTP hydrolysis was determined by means of a decrease in fluorescence at 390 nm. Standard curves with known phosphate concentrations were used to convert the decrease in fluorescence to phosphate production. For the inhibition experiments, BrGTP was added at $t = 0$, and GTP was added after 60 s of baseline data collection.

Data analysis was performed by nonlinear regression using SigmaPlot V8.02 equipped with Enzyme Kinetics Module V1.1 (SPSS Inc., Chicago, IL).

HPLC Studies. After 6 min, aliquots of the GTPase activity and polymerization assay mixtures were frozen in liquid nitrogen, and the nucleotide composition was determined by ion-exchange (reversed-phase) HPLC analysis. Samples (50 μL) were thawed and directly injected into the HPLC system equipped with a Macherey-Nagel CC 125/4 Nucleosil 100-5 C18 HD column (0.5 × 10 cm) and the corresponding guard column and eluted with a linear gradient of buffer A (5 mM $NBu_4H_2PO_4$, 25 mM H_3PO_4/NH_4OH in 95% water/5% acetonitrile, pH 6.3) and buffer B (5 mM $NBu_4H_2PO_4$ in 10% water/90% acetonitrile) at a 0.4 mL/min flow rate. Gradient details: 0−5 min, 0% B; 5−20 min, 0 → 35% B; 20−27 min, 35% B; 27−32 min, 35 → 0% B; 32−35 min, 0% B. Detection: UV absorption at 262 and 253 nm using a Pharmacia LKB VWM2141 dual diode array variable-wavelength detector. Retention times for the different nucleotides were (BrGTP) 23.9 min, (BrGDP) 21.0 min, (GTP) 22.7 min, and (GDP) 18.6 min.

RESULTS

BrGTP (Figure 1) was synthesized in 48% total yield by direct bromination of guanosine in water (*28*) followed by a one-pot triphosphorylation procedure as described (*29*, *30*).

The inhibitory activity of BrGTP was first demonstrated by light scattering and electron microscopy. In contrast to the other experiments described below, electron microscopy was performed in the presence of Ca^{2+}, which stimulates polymer bundling (*31*). Figure 1 shows typical EM images of FtsZ protofilament bundles obtained in the presence of GTP and of different concentrations of BrGTP. Addition of GTP resulted in a large network of protofilament bundles with a mean diameter of 35 ± 7 nm (Figure 1A). When BrGTP/GTP was used in a ratio of 1/4, shorter and thinner bundles (mean diameter 17 ± 3 nm) were formed (Figure 1B). With a 1/2 ratio of BrGTP to GTP, polymerization was further reduced, giving rise to very thin, short filaments with a length of only a few hundreds of nanometers (Figure 1C).

The inhibitory activity of BrGTP was further characterized using a combined assay for both FtsZ polymerization and GTPase activity. In this assay, FtsZ polymerization was followed by 90° angle light scattering on the basis of the method of Mukherjee and Lutkenhaus (*23*) and the GTPase activity of FtsZ was monitored simultaneously by a real-time fluorescence assay for phosphate release (*16*).

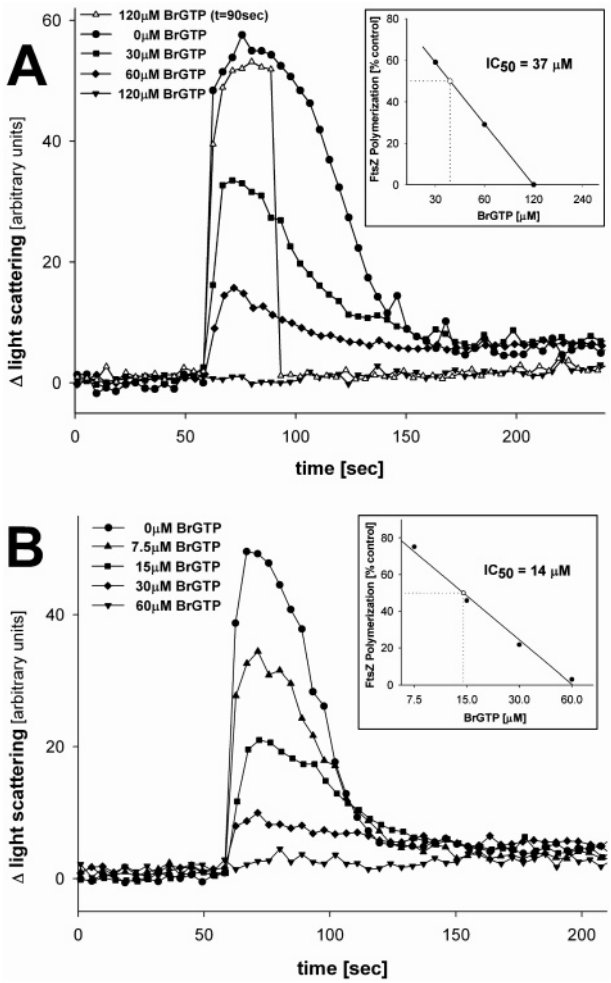

FIGURE 2: Effect of BrGTP on FtsZ polymerization measured by 90° angle light scattering. FtsZ (9 μM) was preincubated for 60 s with different concentrations of BrGTP in HEPES buffer, pH 7.5, at 37 °C, and the assay was started by addition of (A) 60 μM GTP and (B) 30 μM GTP. The IC_{50} value for polymerization was estimated from a semilog plot of the percentage control activity versus BrGTP concentration (see the inset). The maximum change in light scattering upon GTP addition in the absence of BrGTP was set to 100%.

Michaelis−Menten analysis of the rates of GTP hydrolysis at initial GTP concentrations ranging from 7.5 to 120 μM yielded a $K_m = 28.9 \pm 2.8$ μM and a $V_{max} = 4.81 \pm 0.14$ (mol of Pi/mol of FtsZ)/min. The K_m value is comparable with published data (*16*), and also V_{max} is in agreement with those from previous publications (*31*−*33*).

Inhibition experiments with BrGTP were first focused on establishing the mode of inhibition, i.e., reversible, semitight binding, tight binding, or irreversible. As expected, BrGTP itself did not induce FtsZ polymerization, and no phosphate release was observed. Preincubation of FtsZ with BrGTP followed by addition of GTP resulted in the same rate of GTP hydrolysis as addition of the same amounts of BrGTP and GTP as a mixture. Identical results were also obtained when the degrees of polymerization with and without preincubation in the 90° angle light scattering assay were compared. These findings clearly indicate the reversible nature of inhibition by BrGTP.

In the "reverse" experiment, FtsZ (9 μM) was prepolymerized with 60 μM GTP and a 2-fold excess of BrGTP was added at the maximal scattering signal. Within the time

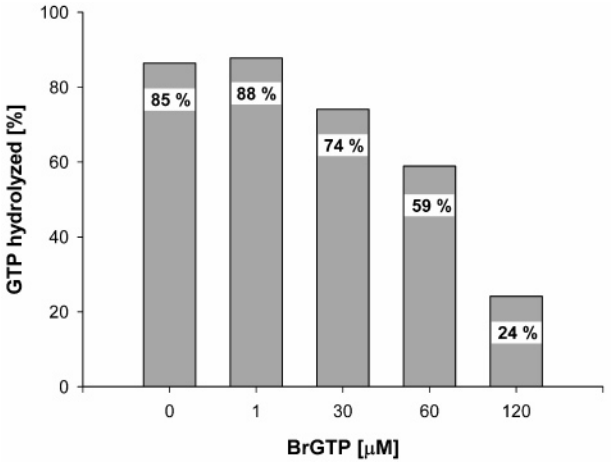

FIGURE 3: Inhibition of FtsZ-catalyzed GTP hydrolysis by BrGTP. After the assays described in Figure 2A were performed, aliquots of the assay mixtures were frozen in liquid nitrogen and the nucleotide composition was analyzed by reversed-phase HPLC.

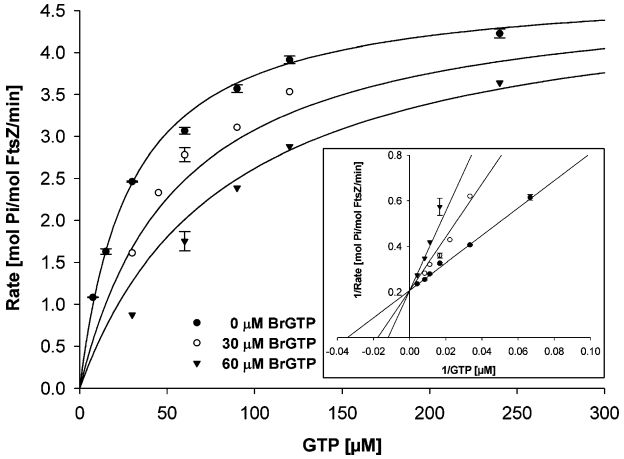

FIGURE 4: Michaelis−Menten and Lineweaver−Burk plots (inset) for FtsZ GTPase activity in the presence of different concentrations of BrGTP. FtsZ (9 μM) was preincubated for 60 s with BrGTP in HEPES buffer, pH 7.5, at 37 °C, and the assay was started by addition of GTP. GTPase activity was measured by a real-time fluorescence-based assay for phosphate release. BrGTP shows the characteristic features of a competitive inhibitor. Nonlinear regression yielded $K_i = 31.8 \pm 4.1$ μM, $K_m = 28.9 \pm 2.8$ μM, and $V_{max} = 4.81 \pm 0.14$ (mol of Pi/mol of FtsZ)/min.

required for the addition of BrGTP (<5 s), GTPase activity was inhibited and light scattering returned to baseline values, indicating complete depolymerization (Figure 2A, open triangles). A control experiment with addition of the same volume of buffer only showed that this result was not simply caused by the addition event itself.

The inhibitory activity of BrGTP for FtsZ GTPase activity was determined from the rates of GTP hydrolysis observed with 60 μM GTP and serial dilutions of BrGTP ranging from 0 to 120 μM. Nonlinear regression analysis yielded $IC_{50} = 60.2 \pm 8.8$ μM. Similar results were obtained for the effect of BrGTP on FtsZ polymerization (Figure 2A). From a semilog plot of the percentage of polymerization (relative to the control without BrGTP) versus the above-mentioned BrGTP concentrations, we estimated $IC_{50} = 37$ μM (Figure 2A, inset). HPLC analysis of the nucleotide composition of the sample mixture after the inhibition experiments (Figure 3) qualitatively confirmed the results obtained with the enzymatic assay for phosphate release. As expected, hydrolysis of BrGTP was generally found to be less than 3%.

The same type of inhibition experiments were also performed with 30 μM GTP and BrGTP concentrations between 0 and 60 μM (Figure 2B). In this case, we obtained IC_{50}(GTPase) $= 26.7 \pm 4.6$ μM and IC_{50}(polymerization) $= 14$ μM. Obviously, the extent of inhibition was not determined by the absolute amount of BrGTP, but by the ratio of BrGTP to GTP. Inhibition experiments with BrGTP in the presence of 120 μM GTP further supported this conclusion (data not shown). Independent of the GTP concentration in our experiments, the IC_{50} for GTPase activity corresponded approximately to a 1/1 ratio of BrGTP to GTP, while it was roughly a 1/2 ratio with respect to polymerization.

To establish the type of reversible inhibition by BrGTP, rates of GTP hydrolysis in the presence of 30 and 60 μM BrGTP were monitored with various initial GTP concentrations. Analysis of experimental data shows that inhibition can be overcome by increasing the substrate concentration, which is indicative of a competitive type of inhibition (Figure 4). Michaelis−Menten analysis of competitive inhibition yielded a $K_i = 31.8 \pm 4.1$ μM.

DISCUSSION

Our results demonstrate the reversible competitive inhibition of FtsZ by BrGTP. In the GTP concentration range studied, the IC_{50} values depend on the ratio of BrGTP to GTP, which is approximately a 1/1 for GTPase activity and 1/2 for assembly. On the first view, BrGTP seems to be more potent in inhibiting FtsZ assembly than its GTPase activity. However, higher BrGTP concentrations result in a larger fraction of shorter FtsZ filaments (see Figure 1). These filaments still possess full GTPase activity but give rise to a comparably low level of light scattering, since light scattering is proportional to polymer mass only when the polymers are longer than the wavelength of the incident light (*23*, *34*). Consequently, the IC_{50} value for assembly obtained by light scattering appears to be lower than the corresponding value for GTPase activity.

A very interesting observation is the complete depolymerization and inhibition of GTPase activity upon addition of a 2-fold excess of BrGTP at the maximum of FtsZ polymerization, which occurs in less than 5 s (the time required for the addition process). Qualitatively, similar results were described in the literature for the addition of GDP at the maximum of FtsZ polymerization (*27*). However, BrGTP proves significantly more active, since a 10-fold excess of GDP still did not lead to complete instantaneous disassembly. In contrast, identical experiments with the nonhydrolyzable GTP analogue guanosine 5′-*O*-(3-thiotriphosphate) (GTP-γ-S) resulted in prolonged polymer persistence (*27*).

Recently, Romberg and Mitchison (*32*) performed a series of ingenious experiments which clarified previously contradictory results in the literature and finally suggested answers to fundamental questions about nucleotide turnover in FtsZ polymers. On the basis of their findings, they proposed a model for the FtsZ polymerization cycle. The main features of this model are (1) GTP hydrolysis is the major rate-limiting step in GTP turnover ($k_{hydrolysis} \approx 8$/min), (2) FtsZ polymers predominantly contain GTP, and only about 20% of polymer subunits contain GDP, and (3) phosphate release

is not rate-limiting, but a step leading to GDP release from the polymer might be partially rate limiting. GDP release may occur either by direct nucleotide exchange in the polymers as suggested by Mingorance et al. (*35*) or via depolymerization and subsequent nucleotide exchange in the monomers. Recent publications provide further evidence for nucleotide exchange in the polymers based on both biochemical data (*14*) and the crystal structure of an *M. jannaschii* FtsZ dimer (*36*).

Our results on the effect of BrGTP on FtsZ polymerization and GTPase activity can be rationalized in terms of Romberg and Mitchison's model. Like GDP, BrGTP alone is not capable to sustain FtsZ assembly under the conditions employed. When FtsZ polymerization is investigated in the presence of both BrGTP and GTP, reduced rates of assembly and GTPase activity are observed. Presumably, BrGTP and GTP compete for binding of soluble FtsZ. In this way, the presence of BrGTP effectively decreases the concentration of soluble FtsZ available for polymerization. The IC_{50} for GTPase corresponding to a 1:1 ratio of BrGTP to GTP suggests that both nucleotides bind with equal affinity and that BrGTP−FtsZ is inactive. In addition, binding of a BrGTP-bound FtsZ monomer to an existing polymer might terminate polymer elongation by blocking assembly of further GTP-bound FtsZ subunits. Finally, BrGTP could also effect polymer destabilization by directly replacing GTP/GDP in the polymers.

This theory can also account for the observation that addition of an excess of BrGTP to preassembled polymers in the presence of GTP results in fast (<5 s) and complete depolymerization and inhibition of GTPase activity. When an excess of BrGTP is added, the pool of GTP-bound soluble FtsZ available for polymerization drastically decreases to a level below the critical concentration for filament formation and GTPase activity, which has been reported to be about 1.5 μM (*14*−*16*). The existing polymers may undergo rapid disassembly via exchange of GTP/GDP for BrGTP in the polymers and/or binding of BrGTP-bound FtsZ to the polymer as described above.

The reason BrGTP-bound FtsZ does not support polymerization is still open to speculation. We assume that either the bulky bromine substituent of BrGTP itself or a conformational change of FtsZ induced upon BrGTP binding prevents association with another FtsZ subunit or destabilizes the polymer in the case of exchange of BrGTP for GTP/GDP in the polymers. In this regard, it is important to note that GTP and BrGTP adopt different conformations in aqueous solutions. While GTP exists primarily in a low anti conformation (*21*), BrGTP prefers a syn conformation, in which the purine base is positioned above the ribose ring (*37*). Since FtsZ-bound GDP is in an anti conformation (*8*), binding of BrGTP might introduce considerable strain. It is imaginable that a correlation exists between the preferred solution conformation of GTP analogues and their affinity and/or effect on FtsZ and tubulin.

Of course, another urgent question has not yet been addressed: What could be the reason for the different effects of BrGTP on the function of FtsZ and tubulin? To answer this question, more structural data on the binding mode of BrGTP in FtsZ and tubulin is required. Ideally, this aim could be achieved by a crystal structure of BrGTP-bound FtsZ. Up to now, it has not been possible to crystallize FtsZ in the presence of GTP or analogues because the polymerization rates with the analogues studied so far are much faster than the crystal growth rates (*36*). The fact that BrGTP does not support FtsZ polymerization circumvents this problem, and adds an extra aspect to the utility of this GTP analogue.

Apart from the direct binding information, which could be provided by a crystal structure, further characterization of the FtsZ−nucleotide interaction can also be achieved by establishing a structure−activity relationship (SAR) with various other GTP analogues. We have recently prepared a series of C8-substituted GTP derivatives and are currently exploring their binding affinities and inhibitory activities for both FtsZ and tubulin.

REFERENCES

1. Romberg, L., and Levin, P. A. (2003) Assembly Dynamics of the Bacterial Cell Division Protein FtsZ: Poised at the Edge of Stability, *Annu. Rev. Microbiol. 57*, 125−154.
2. Carballido-Lopez, R., and Errington, J. (2003) A dynamic bacterial cytoskeleton, *Trends Cell Biol. 13*, 577−583.
3. Addinall, S. G., and Holland, B. (2002) The Tubulin Ancester, FtsZ, Draughtsman, Designer and Driving Force for Bacterial Cytokinesis, *J. Mol. Biol. 318*, 219−236.
4. Den Blaauwen, T., Buddelmeijer, N., Aarsman, M. E., Hameete, C. M., and Nanninga, N. (1999) Timing of FtsZ Assembly in Escherichia coli, *J. Bacteriol. 181*, 5167−5175.
5. Harry, E. J., Rodwell, J., and Wake, R. G. (1999) Co-ordinating DNA replication with cell division in bacteria: a link between the early stages of a round of replication and mid-cell Z ring assembly, *Mol. Microbiol. 33*, 33−40.
6. Margolin, W. (2000) Themes and variations in prokaryotic cell division, *FEMS Microbiol. Rev. 24*, 531−538.
7. Erickson, H. P. (1995) FtsZ, a prokaryotic homolog of tubulin? *Cell 80*, 367−370.
8. Löwe, J., and Amos, L. A. (1998) Crystal structure of the bacterial cell division protein FtsZ, *Nature 391*, 203−206.
9. Nogales, E., Wolf, S. G., and Downing, K. H. (1998) Structure of the $\alpha\beta$ tubulin dimer by electron crystallography, *Nature 391*, 199−203.
10. Löwe, J., and Linda, A. A. (1999) Tubulin-like protofilaments in Ca^{2+}-induced FtsZ sheets, *EMBO J. 18*, 2364−2371.
11. Nogales, E., Whittaker, M., Milligan, R. A., and Downing, K. H. (1999) High Resolution Model of the Microtubule, *Cell 96*, 79−88.
12. De Boer, P., Crossley, R., and Rothfield, L. (1992) The essential bacterial cell-division protein FtsZ is a GTPase, *Nature 359*, 254−256.
13. Scheffers, D.-J., and Driessen, A. J. M. (2001) The polymerization mechanism of the bacterial cell division protein FtsZ, *FEBS Lett. 506*, 6−10.
14. González, J. M., Jiménez, M., Vélez, M., Mingorance, J., Andreu, J. M., Vicente, M., and Rivas, G. (2003) Essential Cell Division Protein FtsZ Assembles into One Monomer-thick Ribbons under Conditions Resembling the Crowded Intracellular Environment, *J. Biol. Chem. 278*, 37664−37671.
15. Mukherjee, A., and Lutkenhaus, J. (1998) Dynamic assembly of FtsZ regulated by GTP hydrolysis, *EMBO J. 17*, 462−469.
16. Sossong, T. M., Jr., Brigham-Burke, M. R., Hensley, P., and Pearce, K. H., Jr. (1999) Self-Activation of Guanosine Triphosphatase Activity by Oligomerization of the Bacterial Cell Division Protein FtsZ, *Biochemistry 38*, 14843−14850.
17. Scheffers, D.-J., de Wit, J. G., den Blaauwen, T., and Driessen, A. J. M. (2002) GTP Hydrolysis of Cell Division Protein FtsZ: Evidence that the Active Site Is Formed by the Association of Monomers, *Biochemistry 41*, 521−529.
18. Margalit, D. N., Romberg, L., Mets, R. B., Hebert, A. M., Mitchison, T. J., Kirschner, M. W., and RayChaudhuri, D. (2004) Targeting cell division: Small-molecule inhibitors of FtsZ GTPase perturb cytokinetic ring assembly and induce bacterial lethality, *Proc. Natl. Acad. Sci. U.S.A. 101*, 11821−11826.
19. White, E. L., Suling, W. J., Ross, L. J., Seitz, L. E., and Reynolds, R. C. (2002) 2-Alkoxycarbonylaminopyridines: inhibitors of Mycobacterium tuberculosis FtsZ, *J. Antimicrob. Chemother. 50*, 111−114.

20. Wang, J., Galgoci, A., Kodali, S., Herath, K. B., Jayasuriya, H., Dorso, K., Vicente, F., González, A., Cully, D., Bramhill, D., and Singh, S. (2003) Discovery of a Small Molecule That Inhibits Cell Division by Blocking FtsZ, a Novel Therapeutic Target of Antibiotics, *J. Biol. Chem. 278*, 44424−44428.
21. Chakrabarti, G., Mejillano, M. R., Park, Y.-H., Vander Velde, D. G., and Himes, R. H. (2000) Nucleoside Triphosphate Specificity of Tubulin, *Biochemistry 39*, 10269−10274.
22. Löwe, J., Li, H., Downing, K. H., and Nogales, E. (2001) Refined Structure of $\alpha\beta$-Tubulin at 3.5 Å Resolution, *J. Mol. Biol. 313*, 1045−1057.
23. Mukherjee, A., and Lutkenhaus, J. (1999) Analysis of FtsZ Assembly by Light Scattering and Determination of the Role of Divalent Metal Cations, *J. Bacteriol. 181*, 823−832.
24. Mukherjee, A., Kai, D., and Lutkenhaus, J. (1993) *Escherichia coli* cell division protein FtsZ is a guanine nucleotide binding protein, *Proc. Natl. Acad. Sci. U.S.A. 90*, 1053−1057.
25. Muraoka, M., Fukuzawa, H., Nishida, A., Okano, K., Tsuchihara, T., Shimoda, A., Suzuki, Y., Sato, M., Osumi, M., and Sakai, H. (1999) The Effects of Various GTP Analogues on Microtubule Assembly, *Cell Struct. Funct. 24*, 101−109.
26. Muraoka, M., and Sakai, H. (1999) Effects of Purinenucleotide Analogues on Microtubule Assembly, *Cell Struct. Funct. 24*, 305−312.
27. Scheffers, D.-J., den Blaauwen, T., and Driessen, A. J. M. (2000) Non-hydrolysable GTP-γ-S stabilizes the FtsZ polymer in a GDP-bound state, *Mol. Microbiol. 35*, 1211−1219.
28. Long, R. A., Robins, R. K., and Townsend, L. B. (1968) 8-Bromoguanosine, in *Synthetic Procedures in Nucleic Acid Chemistry* (Zorbach, W. W., and Tipson, R. S., Eds.) pp 228−229, Wiley International, New York.
29. Halbfinger, E., Major, D. T., Ritzmann, M., Ubl, J., Reiser, G., Boyer, J. L., Harden, K. T., and Fischer, B. (1999) Molecular Recognition of Modified Adenine Nucleotides by the $P2Y_1$-Receptor. A Synthetic, Biochemical, and NMR Approach, *J. Med. Chem. 42*, 5325−5337.
30. Burnstock, G., Fischer, B., Hoyle, C. H. V., Maillard, M., Zinganshin, A. U., Brizzolara, A. L., von Isakovics, A., Boyer, J. L., Harden, K. T., and Jacobson, K. A. (1994) Structure Activity Relationships for Derivatives of Adenosine-5′-Triphosphate as Agonists at P_2 Purinoreceptors: Heterogeneity Within P_{2X} and P_{2Y} Subtypes, *Drug Dev. Res. 31*, 206−219.
31. Yu, X.-C., and Margolin, W. (1997) Ca^{2+}-mediated GTP-dependent dynamic assembly of bacterial cell division protein FtsZ into asters and polymer networks *in vitro*, *EMBO J. 16*, 5455−5463.
32. Romberg, L., and Mitchison, T. J. (2004) Rate-Limiting Guanosine 5′-Triphosphate Hydrolysis during Nucleotide Turnover by FtsZ, a Prokaryotic Tubulin Homologue Involved in Bacterial Cell Division, *Biochemistry 43*, 282−288.
33. RayChaudhuri, D., and Patterson, J. T. (1992) *Escherichia coli* cell-division gene *ftsZ* encodes a novel GTP-binding protein, *Nature 359*, 251−254.
34. Romberg, L., Simon, M., and Erickson, H. P. (2001) Polymerization of FtsZ, a Bacterial Homolog of Tubulin, *J. Biol. Chem. 276*, 11743−11753.
35. Mingorance, J., Rueda, S., Gómez-Puertas, P., Valencia, A., and Vicente, M. (2001) *Escherichia coli* FtsZ polymers contain mostly GTP and have a high nucleotide turnover, *Mol. Microbiol. 41*, 83−91.
36. Oliva, M. A., Cordell, S. C., and Löwe, J. (2004) Structural insights into FtsZ protofilament formation, *Nat. Struct. Mol. Biol. 11*, 1243−1250.
37. Sarma, R. H., Lee, C.-H., Evans, F. E., Yathindra, N., and Sundaralingam, M. (1974) Probing the Interrelation between the Glycosyl Torsion, Sugar Pucker, and the Backbone Conformation in C(8) Substituted Adenine Nucleotides by ^1H and ^1H-{^{31}P} Fast Fourier Transform Nuclear Magnetic Resonance Methods and Conformational Energy Calculations, *J. Am. Chem. Soc. 96*, 7337−7348.

BI047297O